Experiment 9: Gamma spectroscopy Phyical advanced practical course

Group F 24 Leonard
Käferstein () Jakob
Adamczewski ()

Carried out on: 19.10.2021

Summary

In this experiment, high-resolution gamma spectroscopy is carried out with the aid of a germanium semiconductor detector. First, the most important physical mechanisms are described. Then the results of the laboratory experiment are presented and analyzed. The gamma activity of the room background was measured and traced back to known sources. The gamma spectrum of two unknown samples and an old fluorescent miner's clock made with radium were also determined. The measured *γ-radiation activities* could thus be traced back to their decays and certain components of the samples could be determined. The samples contain uranium-238 and thorium-232 and can therefore possibly be traced back to uranium ore for sample 1 and monazite phosphocei for sample
2 can be traced back. Further research would be required to determine this more precisely. The experiment thus provides an insight into the many possible applications of gamma spectroscopy.

1 Introduction

Gamma spectroscopy examines the intensity and energy of gamma radiation. This is produced when atomic nuclei are highly energized after radioactive decay. In order to move to a lower energy level, energy is released in the form of a gamma particle.
This interacts in various ways with the electrons of a germanium semiconductor detector and releases them from their band structure. The electrons released by the interaction processes can now be measured and allow conclusions to be drawn about the energy of the gamma particle. As the energy is characteristic of decay and the atoms involved, the elements present can be determined. Both the quantum mechanical interpretation of light and the consideration of photons and electrons as classical particles are used to explain these processes.

1.1 Theoretical foundations

The function of the semiconductor detector is described below, together with the underlying physical mechanisms and the interactions of gamma particles with the electrons in the detector.

1.1.1 Semiconductors

The semiconductor germanium is used in the detector. This forms a crystal structure and therefore a lattice in which the valence electrons are located. More detailed information on this can be found under 1.3.1. Electrons are transported from the valence band to the conduction band by supplying energy, for example through collisions or photons, but a certain energy E_B is required for this. (See Fig. 1) In experiments, this is mainly caused by gamma photons (also known as gamma particles). These act through the physical effects described in 1.1.2 to 1.1.4, whereby the photon energy is emitted. The higher the energy of the photon, the more electrons are affected and the more energy is emitted[4].

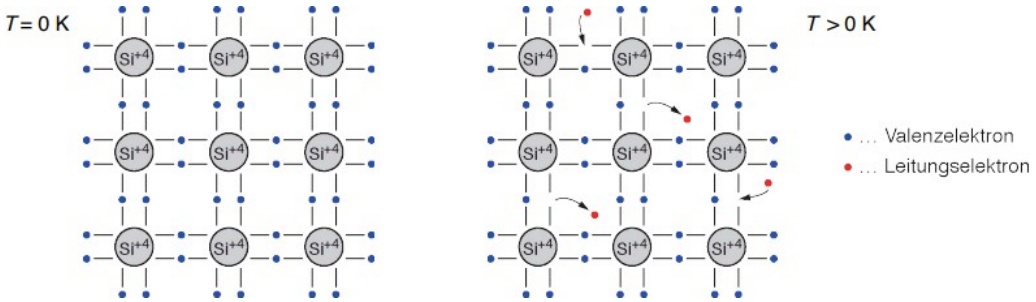

Source: https://tinyurl.com/tcypxd42 20.10.2021

Figure 1: Electrons in the crystal lattice, using silicon as an example. The effect is the same for silicon and germanium

However, it is also possible that the electrons are transported from the valence band into the conduction band by other effects, including the quantum mechanical tunnel effect, which arises due to the fundamental statistical nature of quantum mechanics. More detailed information on the tunnel effect can be found in the literature (e.g. Demtroder Wolfgang. "4.3.1 Tunnel effect." *Experimental Physics 3* [4]).

These effects are more pronounced when there is generally more thermal energy and the electrons are in higher energy states. The semiconductor is cooled with liquid nitrogen to minimize these effects and return the electronless solution to gamma radiation.

1.1.2 Photoelectric effect

The photoelectric effect causes the "full energy peak" (FEP) that we are investigating (see Fig. 2). This effect was first described at the beginning of the 20th century and was enormously important in the development of quantum theory and can be described in simplified terms as follows. A photon is absorbed by an electron and emits its entire energy E_P to the electron and releases it from its bond, in the case of the semiconductor from the valence band. The

The sum of the energy E_B and the kinetic energy E_{kin} results in E_P .

$$E_P = E_{kin} + E_B \tag{1}$$

The higher the kinetic energy of the electrons, the higher the energy measured later. As the energy of the photon is available in quantized form, conclusions can be drawn about the energy of the original photon.

$$E_P = h\nu = \frac{hc}{\lambda} \tag{2}$$

Here we use this effect to measure the γ photon.

1.1.3 Compton effect

In the Compton effect, the photon is scattered by the electron. The process can be regarded as an elastic collision due to wave-particle duality.

$$E^2 = (m\ c\ )_0{}^{22} + p\ c^{22}\ \frac{hc}{\lambda}\ ^2 \tag{3}$$
$$=$$

If the photon has a momentum and an electron has the Compton wavelength $\lambda_c = \frac{h}{m}$, which changes by $\Delta\lambda_c$ due to the elastic impact, c_0

$$\Delta\lambda_c = \frac{h}{m\ c_0}(1 - \cos\theta) \tag{4}$$

where θ is the scattering angle, the energy of the photon E^r changes to γ

$$E^r(\theta) = \frac{E_\gamma}{1 + \frac{E\gamma}{m_e c^2}(1 - \cos\theta)}. \tag{5}$$
γ

For a more detailed derivation, please refer to the literature (e.g. Demtroder Wolfgang. "3.1.6 Compton effect." *Experimental Physics 3* [4]).

This is expressed in the measurement by a kind of plateau, the so-called Compton continuum (C.K.), from which other peaks protrude, as the gamma particles do not release their entire energy.

For $\theta > 180$, the maximum energy output is reached and the Compton continuum drops sharply at the so-called Compton edge (C.E). Nevertheless, further inaccuracies arise when the scattered gamma particle hits an electron again [10]. (See Fig. 2)

1.1.4 Pair Production

Particularly high-energy gamma photons have enough energy to generate a pair of electron and positron on arrival. This requires at least the rest energy of the two particles $E_P = 2m\ c_e^2 \approx$ 1022 keV, excess energy is converted into kinetic energy E_{kin}.

The positron, as the antiparticle of the electron, encounters an electron again after a very short time, causing both particles to disappear. This produces two photons with $E_P = m\ c_e^2 \approx$ 511 keV.
Three processes can now take place (see Fig. 2)

1) ***SingleEscape*** **:** A photon leaves the detector without interaction, secondary peak (SEP) appears at 511 keV.
2) ***DoubleEscape*** **:** Both photons leave the detector without interaction, secondary peak (DEP) appears at 1022 keV.
3) ***NoEscape*** **:** Both photons interact in the way already described, the energy falls into the main peak (FEP).

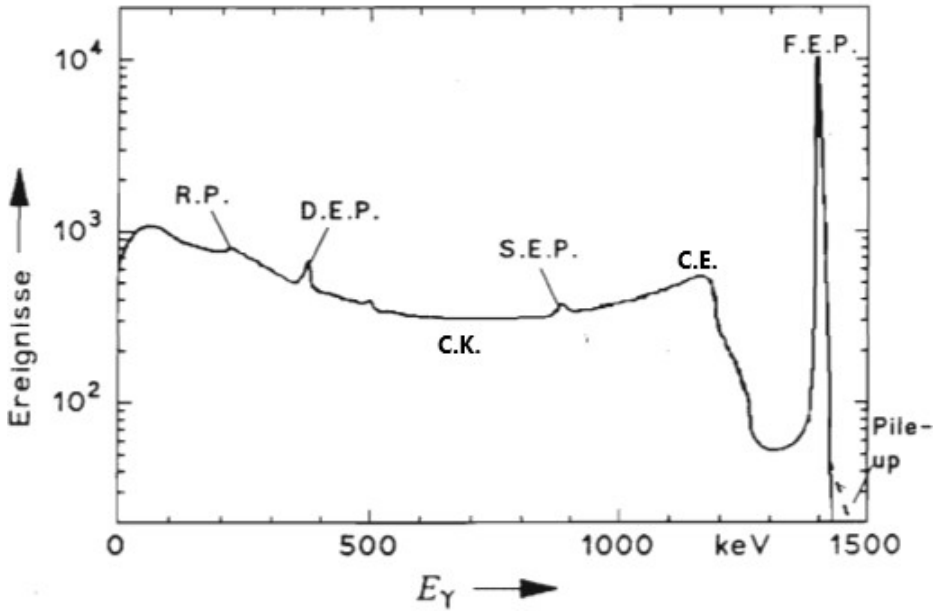

Source: https://tinyurl.com/ny5wxt4c 20.10.2021

Figure 2: Exemplary gamma ray energy spectrum with b escribed characteristics

1.1.5 Gamma radiation and decay chains

Three different decay chains occur in nature. These begin with the very heavy atoms ^{238} U, ^{235} U and ^{232} Th and then gradually decay into other atoms. This occurs through alpha decay, in which a He nucleus is released, beta plus decay, in which a proton decays into a positron and a neutron, and beta minus decay, in which a neutron decays into an electron and a proton.

After decay, the atomic nucleus is energetically in a highly excited state. This energy is usually released by the emission of a gamma photon, which is the subject of our measurement. The atom either emits the entire energy at once, or it passes through intermediate stages with smaller energy jumps. Since beta decay is not energetically discrete, lower energy levels can also be assumed directly after decay.
Figure 3 shows this for the *β-decay of* cobalt to nickel. The arrows drawn in the figure are labeled first with the relative frequency of the individual excitation processes and in bold the energy emitted in the form of a gamma photon. Next to the energy levels are the lifetimes of these.

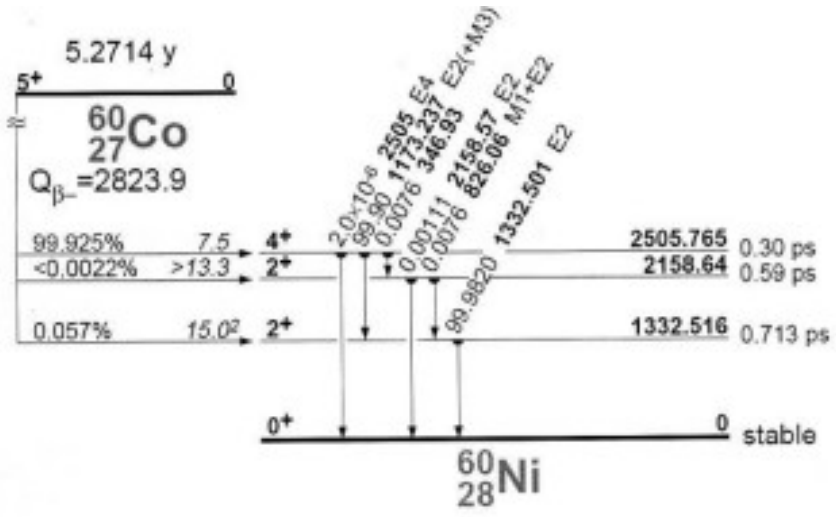

Source: https://tinyurl.com/37anyxw7 20.10.2021

Figure 3: Level diagram of the states assumed in^{60} Ni after the decay of^{60} Co, and release of energy by gamma particle emission

According to the principles of quantum mechanics, the energy of a photon is present in quantized form. This is a multiple of the frequency v, multiplied by Planck's quantum of action h:

$$E_{Ph} = hv = \frac{hc}{\lambda} \tag{6}$$

As the energy emitted by the excited atom is very high, the photons have very high frequencies or energies. Due to the way these photons are generated, they are also referred to as gamma radiation.
The energy of the gamma particle is characteristic of the decay. This allows us to draw conclusions about the parent atoms and the decay series.

More detailed information can be found in the tables in the test instructions [8].

1.2 Experimental setup

1.2.1 Structure of the detector

The detector consists of several layers of germanium, one on top of the other. A voltage is applied to the layers to transport the released electrons to an amplifier and then to a multi-channel analyzer. The more energetic the gamma particles are, the deeper they penetrate and the more energy the released electrons have. The energy between 0 keV and 3000 keV can be resolved via 8192 channels. At the opening there is a cap made of a metal, in this case beryllium, to control the entry of radiation. The entire detector is placed in a liquid nitrogen container for cooling purposes (see 1.1.1).

1.2.2 Calibration

In order to correlate the detector channels with the energy and intensity of the radiation, Cs-137 is used to measure both the applied voltage and the shape time constant

calibrated. These influence the detection accuracy but also signal noise. The shape time constant (also known as the rise time) refers to the time intervals in which the discrete events are recorded. Rapid decay avalanches can occur, especially with strongly ionizing radiation, which is why a higher rise time should also lead to a better resolution. Pile-ups can occur if the rise time settings are too high. The dead time of the detector, i.e. the time between two signal pulses during which nothing is detected, can also increase.

The quantity to be measured is the activity of the nuclide in question in the sample. If one of these variables is to be determined absolutely, the counting yield of the detector must be calibrated as a function of the gamma energy.
To do this, the channel number of the detector is adapted to the energy of the gamma particles, for which samples with known gamma radiation energy are used (^{137} Cs,^{22} Na,^{60} Co). Frequently, known peaks from the background such as^{40} K are also used for this purpose.

1.2.3 Measurement and background radiation

Since we want to determine the composition of unknown samples, it is necessary to exclude contamination by background radiation and other gamma emitters such as potassium-40. For this purpose, the background radiation of the laboratory is measured over a certain period of time. The peaks of the background radiation can then be disregarded in the main measurement in order to obtain the gamma spectrum of the samples. Certain energy peaks can be read from this spectrum and assigned to the various elements using nuclide maps.
An intensity-half-life ratio could also be used to draw conclusions about the quantitative composition of elements in the sample. This requires a correlation between the measured intensity of the radiation and the actual radiation released from the sample.

1.3 Materials used

1.3.1 Germanium crystal structure

Germanium is a semiconductor from the same main group as silicon. The two elements share many properties, such as the formation of a diamond-like crystal structure (see Figure 4). This structure also determines the electrical conductivity of the semiconductor.

In a conductor, the valence electrons of the bonds between the atoms (usually pi-molecule bonds) are located in the crystal lattice in the so-called valence band. When electrons are released from this band and brought into the conduction band, holes are created which can be occupied by other electrons, resulting in electrical conductivity. (See Figure 5)

In a semiconductor, this transition is not smooth, but requires energy, as the conduction and valence bands are energetically separated. The transition to an insulator is smooth here.

In our experiment, this energy is added by the gamma particles. Germanium detectors have the advantage that they are very precise and have a high detection resolution, but require cooling.

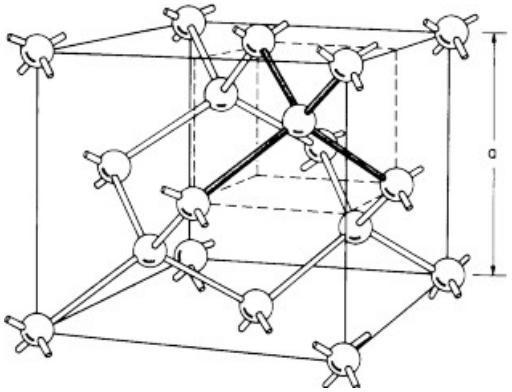

Source: https://tinyurl.com/tcypxd42 20.10.2021

Figure 4: Diamond structure

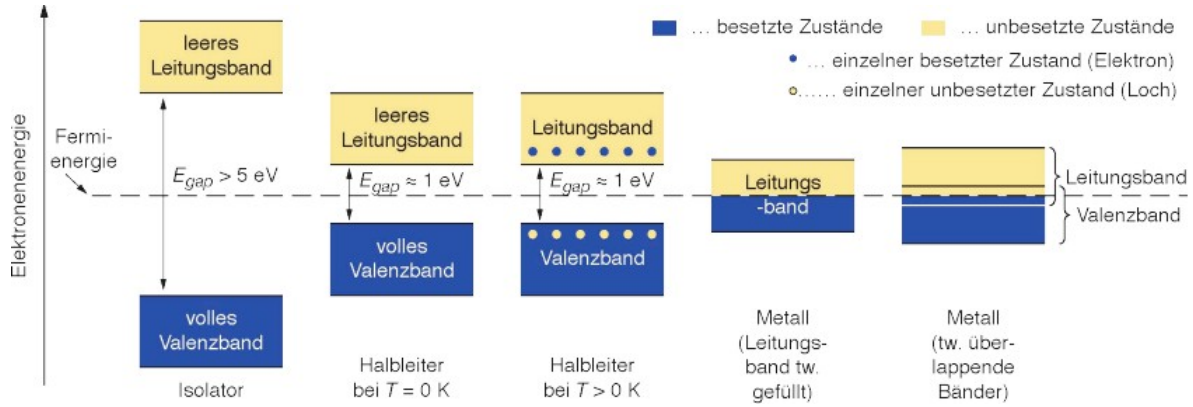

Source: http://www.chemgapedia.de/vsengine/vlu/vsc/de/ch/16/ ac/elemente/vlu/32.vlu.html 20.10.2021

Figure 5: Valence and conduction band

1.3.2 Radiation sources

The substances used for calibration ^{137}Cs, ^{22}Na and ^{60}Co are suitable for the task, as there is a very high probability that the same decay with known emission energies will occur frequently. In addition, we expect the occurrence of the 1461 keV peak of ^{40}K, a nuclide found in biological substances, and the 511 keV peak of cosmic background radiation in the background measurement. Depending on the geographical location, radon, residues of radioactive radiation released in Chernobyl and other radioactive minerals may also occur.

2 Results and discussion

2.1 Adjusting and calibrating the spectrometer

We investigate the resolving power of the energy peaks $R = \frac{FWHM}{E_{Peak}}$ to find a maximum in the resolution accuracy, we measure a ^{137}Cs sample and its energy peak and apply these as a function in order to find a maximum. The FWHM is given in hundredths of a channel width.
First, we apply the operating voltage of the detector, which we increase from *1300V* to *2500V* increase. The measuring time is *180s*, the rise time is constant at *2µs*

The relationship between resolution and voltage results in the relationship shown in Fig. 6. Consequently, we select *2500V* as the operating voltage, as the peak width is sharpest here.

Now we repeat the same with the rise time, which we increase in 1.*6µs* steps from 0.*5µs* to *12µs,* whereby we record the voltage at the previously found point of *2500V*. The measurement duration is *120s*, then we calculate the same ratio as before. The relationships are shown in Fig. 6. The most precise peaks are obtained with the highest rise time of *12µs*.

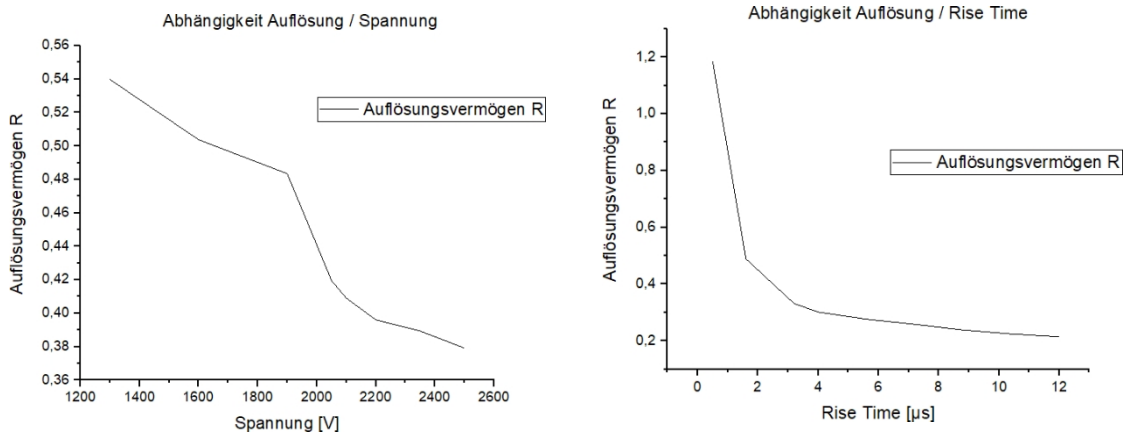

Figure 6: Dissolution capacity

Finally, we calibrate the scale of the detector by measuring the known energy of the elements^{137} Cs,^{22} Na and^{60} Co, which has two lines, and perform a linear fit with the channel number. (See Fig. 8 and Table 1)

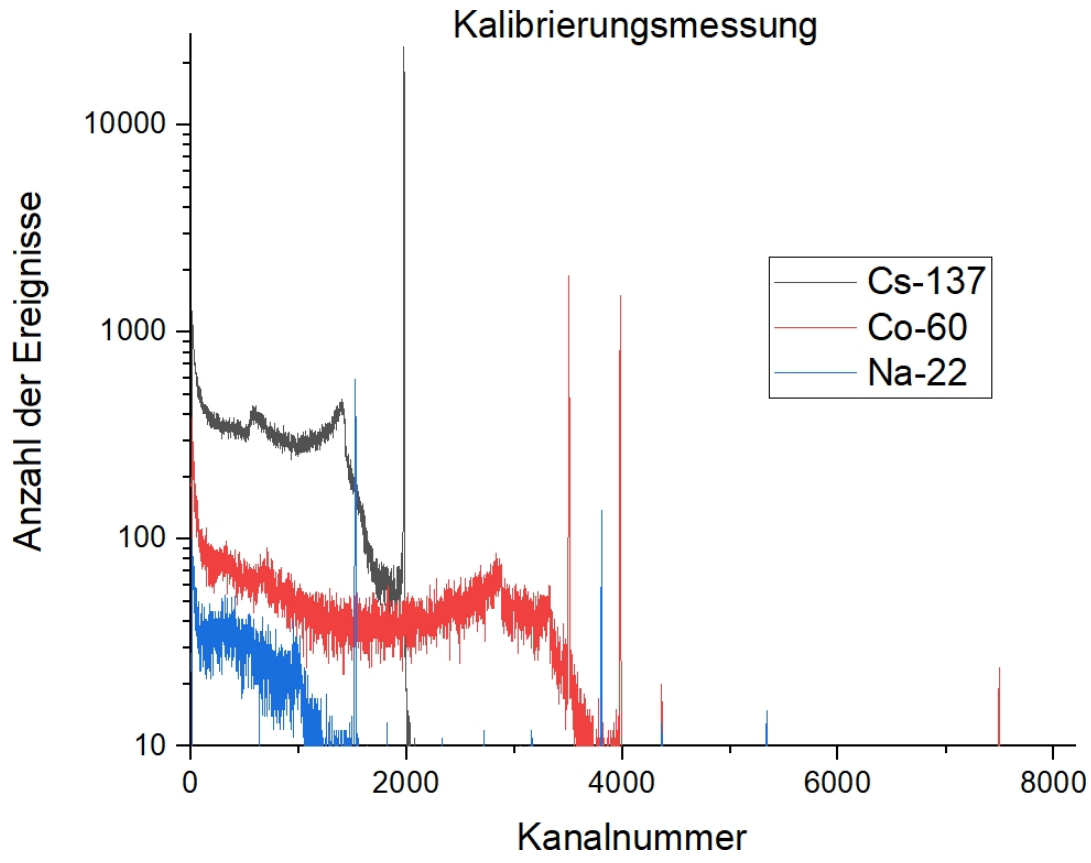

Figure 7: Calibration measurement. The y-ac hse was set to 10 counts to eliminate unnecessary noise.

Two peaks are recognizable when measuring sodium. Here we disregard the significantly larger peak at 511 keV, as this is the SEP of pair production [6]. Since the SEP also has this unique energy, the peak could of course also be used for calibration, but we have refrained from doing so.

Fig. 7 shows the respective clearly assigned peaks of the three elements. These were measured on channel numbers 1977, 3506, 3809 and 3983. These channel numbers were then assigned the energies known from the literature for the respective peaks, i.e. 662keV for ^{137} Cs, 1173keV and 1333keV for ^{60} Co, and 1275keV for ^{22} Na. With the linear fit shown in Fig. 8, the corresponding energy can be assigned to each channel. Photons with energies up to almost 3MeV can thus be detected very accurately by the measurement aperture.

Isotope	Energy [keV]	Channel number
^{137}Cs	662	1977
^{60}Co	1173	3506
^{22}Na	1275	3809
^{60}Co	1333	3983

Table 1: Energy calibration values

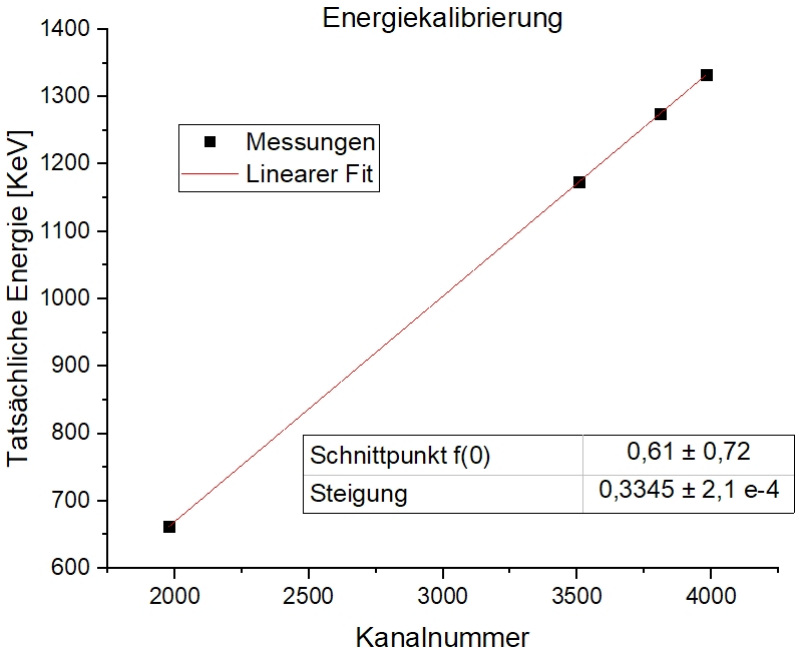

Figure 8: Linear fit for energy calibration

2.2 Background measurement

In order to know the background radiation and thus to be able to subtract it from the other measurements , it is measured in the laboratory over a period of 30 minutes and interestingly identified. The isotopes occurring can be found using the tables from the literature of the task [8]. The isotopes identified are listed in Table 2 and Fig. 9. The peaks of the pair production of the decay of thalium are also shown as an example.

Of particular note here are ^{40} K, as this does not originate from natural decay series but from cosmic radiation and is therefore very common in nature and living organisms, and ^{137} Cs, which was released into the environment primarily as a result of the Chernobyl reactor disaster and nuclear weapons tests. The contribution of anthropogenic radiation sources in the Leipzig region is therefore rather low, which is consistent with the spread of radiation after the reactor disaster.
The radioactive gas ^{222} Rn is barely recognizable in the measurement. It is produced by decay processes in the rock and rises through it, often collecting in cellars, which can pose a significant health risk. The fact that radon hardly ever occurs is partly due to the location of the laboratory on the second floor, good ventilation, but also the low occurrence of radon in the Leipzig region. However, this is not the case in the nearby low mountain ranges of the Thuringian Forest, Fichtelgebirge and Erzgebirge.

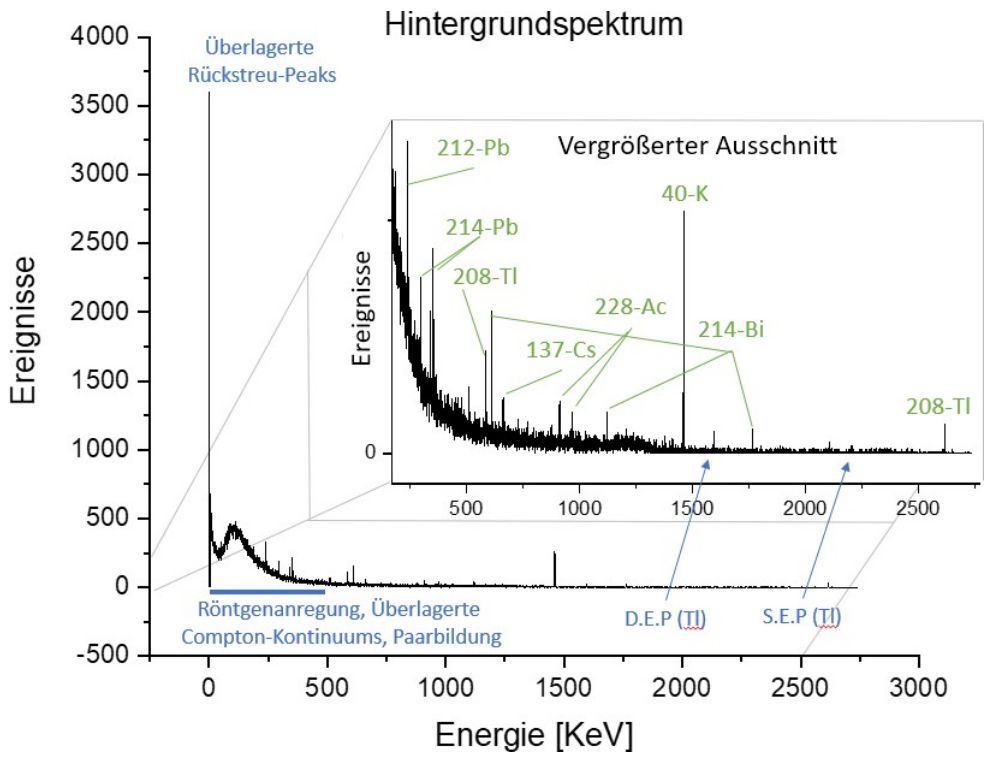

Figure 9: Background measurement. At the top right is the enlarged section without the backscatter peak, labeled with the original nuclides.

Energy [keV]	Forming isotope	Mother isotope	Notes
2616	^{208}Pb	^{208}Tl	^{232}Th series
2104	-	-	Single Escape of the Pair Production of the Thallium
1765	^{214}Po	^{214}Bi	^{238}U-series (via Radon)
1592	-	-	Double escape of the pair production of the thallium environment and living beings
1461	^{40}Ar	^{40}K	^{238}U-series (via Radon)
1120	^{214}Po	^{214}Bi	^{232}Th series
968	^{228}Th	^{228}Ac	see above
911	^{228}Th	^{228}Ac	Chernobyl
661	^{134}Ba	^{137}Cs	^{238}U-series (via Radon)
609	^{214}Po	^{214}Bi	^{232}Th series
583	^{208}Pb	^{208}Tl	^{238}U-series (via Radon) see above.
351	^{214}Bi	^{214}Pb	^{232}Th series
295	^{214}Bi	^{214}Pb	
238	^{212}Bi	^{212}Pb	

Table 2: Notable nuclides of the background measurement

2.3 Natural sample

We use an old miner's watch as a natural sample. To make it easier to read in the dark, this was given a fluorescent coating, which is excited by a radioactive substance. As a rule, radium salt was used for this purpose. The use of radium was common until the 1960s, and for much longer in military applications, making all watches with a fluorescent coating a potential health risk [3]. We record the radiation from the watch for 20 minutes. We then subtract the background spectrum, which is set in relation to time. The results are shown in Table 3 and Fig. 10.

The sample mainly contains nuclides from the ^{238}U series. Since it was produced from the same material, which decays over time, this is to be expected. The initial nuclide is in fact radium, which decays to ^{222}Rn with a half-life of 1630 years and causes the peak at 168 keV. The remaining decays have half-lives of days to minutes and usually have a significantly lower intensity and energy. The short half-lives lead to a rapid end of the decay chain for the stable ^{206}Pb.

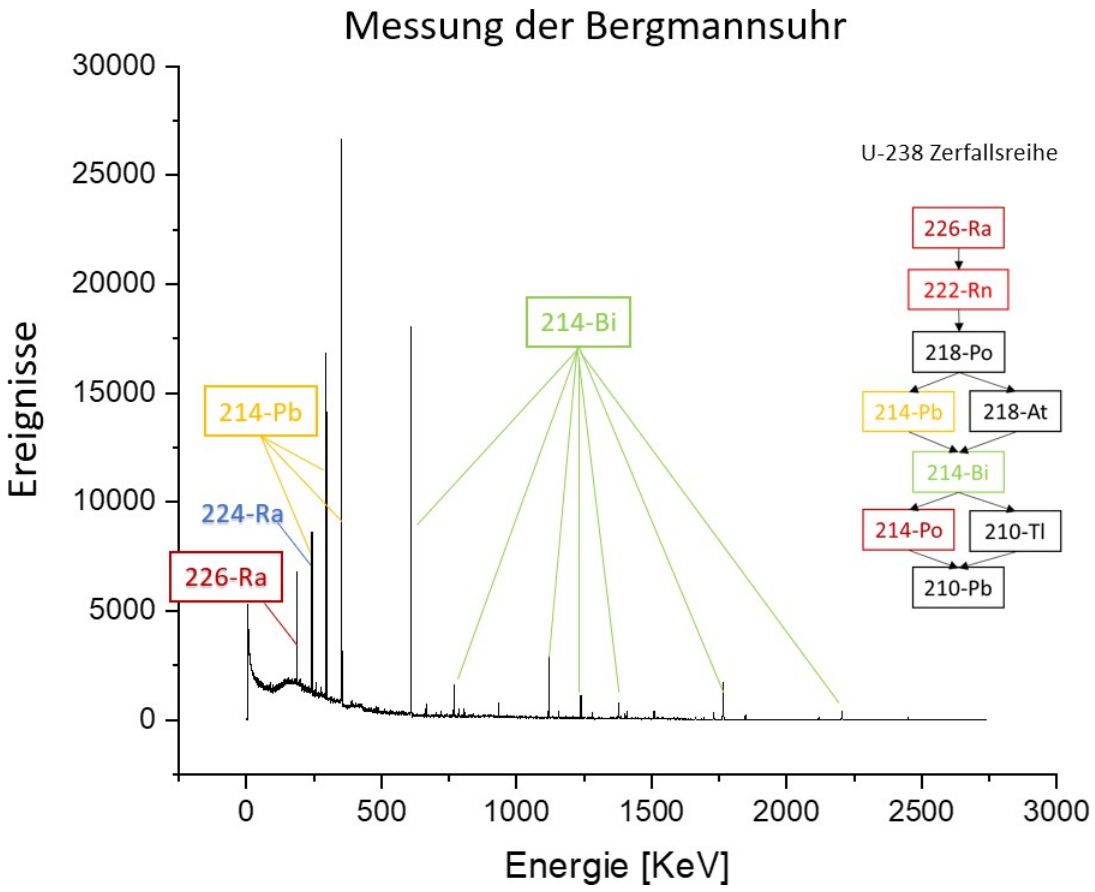

Figure 10: Notable nuclides in the miner's watch

Energy [keV]	Forming isotope	Mother isotope	Notes
186	^{222}Rn	^{226}Ra	^{238}U-decay series
241	^{220}Rn	^{224}Ra	^{232}Th decay series
242	^{214}Bi	^{214}Pb	^{238}U-decay series via Rn^{222}
295	^{214}Bi	^{214}Pb	
351	^{214}Bi	^{214}Pb	
609	^{214}Po	^{214}Bi	^{238}U-decay series via Rn^{222}
768	^{214}Po	^{214}Bi	
1120	^{214}Po	^{214}Bi	
1238	^{214}Po	^{214}Bi	
1378	^{214}Po	^{214}Bi	
1765	^{214}Po	^{214}Bi	
2204	^{214}Po	^{214}Bi	

Table 3: Notable nuclides of the watch

2.4 Unknown samples

2.4.1 Sample 1

The gamma spectrum of two unknown samples was measured. The procedure was the same as for the measurement of the Bergmann clock. The energy peaks were assigned to nut nuclides and labeled. Fig. 11 shows this for sample 1 and Fig. 12 for sample 2. Table 4 lists the exact energies with nut nuclide, nuclide produced and associated decay series for sample 1. In Table 5 for sample 2.

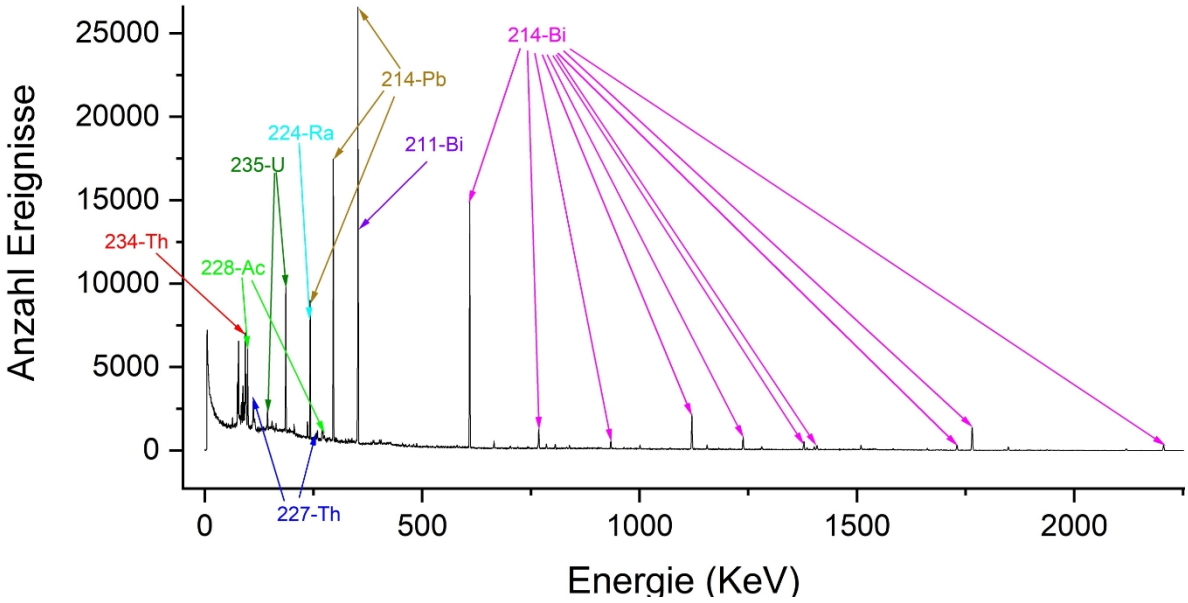

Figure 11: Specific nuclides of sample 1

The gamma spectrum is characteristic of that of uranium ore [5]. It can be said with certainty that sample 1 contains uranium. In particular, the^{238} U decay series is to a large extent

can be found in the spectrum. The ^{238} U decays to ^{234} Th and this decays further to ^{234} Pa. For this decay there was the 92.6 keV peak as an indication of its existence. From here it continues to ^{234} U, detected with the 1001 keV peak. The decays from ^{230} Th onwards to ^{218} Po have left no traces in the gamma spectrum. However, the subsequent decays of ^{214} Pb to ^{214} Bi (242 keV, 295 keV and 352 keV) and of ^{214} Bi to ^{214} Po (609 keV, 768 keV, 934 keV, 1120 keV, 1239 keV, 1378 keV, 1408 keV, 1729 keV, 1765 keV and 2204 keV).
Some of the events found can be traced back to the ^{235} U decay chain. Every peak that could be assigned is noted in Table 4.
Figure 11 also clearly shows the Compton Plateau up to about 260 keV, from which various other energy peaks stand out.
Most of the FEPs in the spectrum are too low in energy to produce an SEP or even a DEP. Almost all peaks of the spectrum could be assigned to decays of the ^{238} U decay series. False assignments are therefore extremely unlikely. The assignment to uranium also fits very well because the sample itself had the somewhat dirty yellow color known from uranium ore.

Energy [keV]	Forming isotope	Mother isotope	Notes
92.6	^{234}Pa	^{234}Th	^{238}U- decay series
99,6	^{228}Th	^{228}Ac	^{232} Th- decay series
113,1	^{223}Ra	^{227}Th	^{235} U- decay series
143,8	^{231}Th	^{235}U	^{235} U- decay series
185,7	^{220}Rn	^{235}U	^{232} Th- decay series
241	^{214}Bi	^{224}Ra	^{238} U- decay series
242	^{223}Ra	^{214}Pb	^{235} U- decay series
256	^{219}Rn	^{227}Th	^{235} U- decay series
269	^{228}Th	^{223}Ra	^{232} Th- decay series
270	^{215}Po	^{228}Ac	^{235} U- decay series
271	^{214}Bi	^{219}Rn	^{238} U- decay series
295	^{207}Tl	^{214}Pb	^{235} U- decay series
351	^{214}Bi	^{211}Bi	^{238}U- decay series via Rn^{222238}
352	^{214}Po	^{214}Pb	U- decay series via Rn^{222238} U-
609	^{214}Po	^{214}Bi	decay series via Rn^{222238} U-
768	^{214}Po	^{214}Bi	decay series via Rn^{222238} U-
934	^{234}U	^{214}Bi	decay series
1001	^{214}Po	^{234m}Pa	^{238}U- decay series via
1120	^{214}Po	^{214}Bi	Rn^{222238} U- decay series via
1238	^{214}Po	^{214}Bi	Rn^{222238} U- decay series via
1378	^{214}Po	^{214}Bi	Rn^{222238} U- decay series via
1408	^{214}Po	^{214}Bi	Rn^{222238} U- decay series via
1729	^{214}Po	^{214}Bi	Rn^{222238} U- decay series via
1765	^{214}Po	^{214}Bi	Rn^{222}
2204		^{214}Bi	

Table 4: Nuclides of the peaks found in the measurement of sample 1

2.4.2 Sample 2

The gamma spectrum of sample 2 clearly shows all signs of a ^{232} Th decay chain. The first two steps of this decay from ^{232} Th to ^{228} Ra and then ^{228} Ac do not cause any measurable gamma photons. the subsequent decays (^{228} Ac $\rightarrow$ ^{228} Th $\rightarrow$ ^{224} Ra $\rightarrow$ ^{220} *Rn* $\rightarrow$ ^{216} Po $\rightarrow$ ^{212} *Pb* $\rightarrow$ ^{212} Bi $\rightarrow$ ^{212} Po) can all be deduced from the spectrum. The measurement has exactly this result. Since thorium-232 has a very long half-life of 1.4 - 10^{10} years, but the next decay to radium-228 is only 5.75 years and the first measurable decay of actinium-228 is only 6.15 hours, we assume that the higher decays also take place in any case. Otherwise the sample could not be stored for a longer period of time without the decay spectrum changing significantly. For these reasons, we assume in the further discussion that the sample actually contains thorium-232.
A detailed list of the energy peaks found is given in Table 5.
Events caused by the Compton effect could also be recorded here. However, apart from the Compton continuum and the backscatter peak, a known event can also be found for the 511keV SEP of pair production.

A closer look at a comparative gamma spectrum from the literature [9] confirms the analysis with the result that it is thorium-232.
In the comparison spectrum, the thorium was located in an incandescent mantle of a gas lamp. Sample 2, however, was present as a sand-like substance of white color. Since thorium is currently a common waste product in the extraction of rare earths, where it occurs in the form of monazite sand (mixed phosphate with 5-10% thorium) [7], it is assumed that it is precisely this sand. However, monazite sand often has a darker brownish color. The same applies to thorite, while thorianite has a more dark metallic appearance.
Ore monazite powder (monazite phosphoceite) is sold online [1] in the form we knew it from the laboratory. We therefore suspect that it could be such a powder. However, in order to be able to determine this exactly, further research would have to be carried out which would go beyond the scope of the experiment.

Figure 12 and Table 5 clearly show that sample 2 is very rich in thorium-232.

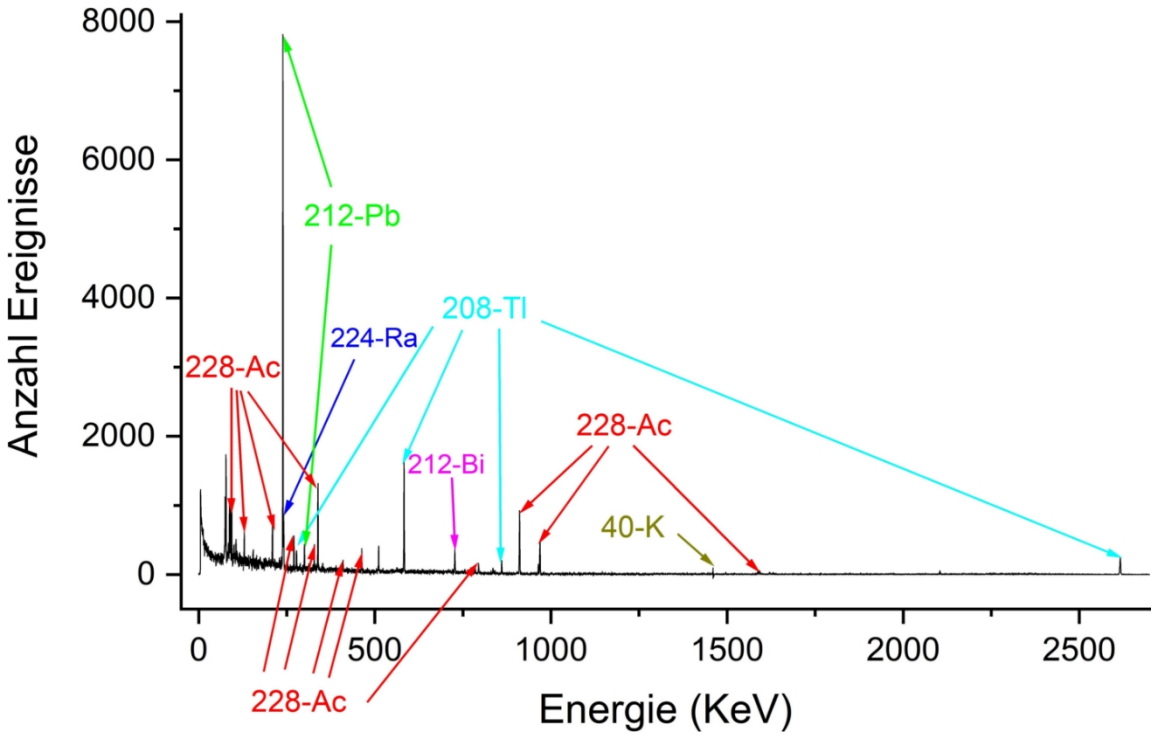

Figure 12: Certain nuclides of sample 2

Energy [keV]	Forming isotope	Mother	Notes X-Ray
87.3	^{234}Pb	isotope	^{232}Th decay series
92,6	^{228}Th	-	^{232}Th- decay
129,1	^{228}Th	^{228}Ac	series^{232} Th- decay
209,3	^{228}Th	^{228}Ac	series^{232} Th- decay
238,6	^{212}Bi	^{228}Ac	series^{232} Th- decay
241	^{220}Rn	^{212}Pb	series^{232} Th- decay
270,2	^{228}Th	^{224}Ra	series^{232} Th- decay
277,4	^{208}Pb	^{228}Ac	series^{232} Th- decay
300,1	^{212}Bi	^{208}Tl	series^{232} Th- decay
328	^{228}Th	^{212}Pb	series^{232} Th- decay
238,3	^{228}Th	^{228}Ac	series^{232} Th- decay
409,5	^{228}Th	^{228}Ac	series^{232} Th- decay
463	^{228}Th	^{228}Ac	series
511	-	^{228}Ac	Doppler broadening positron annihilation
583,2	^{208}Pb	-	^{232}Th- decay
727,3	^{212}Po	^{208}Tl	series^{232} Th- decay
794,9	^{228}Th	^{212}Bi	series^{232} Th- decay
860,6	^{208}Pb	^{228}Ac	series^{232} Th- decay
911,2	^{228}Th	^{208}Tl	series^{232} Th- decay
964,8	^{228}Th	^{228}Ac	series^{232} Th- decay
969	^{228}Th	^{228}Ac	series^{232} Th- decay
1460,8	^{40}Ar	^{228}Ac	series
1588,2	^{228}Th	^{40}K	Randomly stronger background
2614,5	^{208}Pb	^{228}Ac	^{232}Th decay series
		^{208}Tl	^{208}Pb

Table 5: Nuclides of the peaks found in the measurement of sample 2

2.5 Error analysis

Not all photons were detected exactly at the energy stated in the literature. Of course, an enormous number of factors play a role here.
As an example, the energies determined during the measurement of sample 2 were compared with the literature values. This results in a standard deviation of 0.43 keV with the mean at 0.2 keV and an average deviation of 0.38 keV. These values are indeed very accurate and justify the name of high-resolution spectroscopy.
The hardware manual of the detector contained some information on the uncertainty, which, however, also depends on many factors [2].
Before the start of the experiment, we expected a maximum error of up to 2.5 keV and an average deviation of around 0.5 keV to 1 keV. In both cases, reality e x c e e d s expectations.
Causes for measurement uncertainties can be errors during calibration, the fact that 3000 keV was divided into only 8192 channels, which means a maximum resolution of 0.37 keV steps.
Apart from this, inaccuracies can also be caused either by the angle of incidence of the radiation, thermal noise, pile ups or dead times of the detector. Small disturbances can also occur in the electronics which are not always easy to calculate.

3 Summary and outlook

Nuclides from natural decay chains were mainly present in the background measurement. An exception to this is ^{40}K and ^{137}Cs, whereby we can conclude from the intensity of the latter that the Leipzig region has a rather low exposure to anthropogenic radioactivity. The experiment also took place in a laboratory where radioactive substances are used more frequently. Just ^{137}Cs was still on the detector until shortly before the start of the measurement.
The discovery of the naturally occurring radioactive gas ^{22}Rn also has anthropogenic origins. This is released by decay processes in the rock. Both measured values are consistent with the expected radioactive contamination.

As expected, the miner's watch is also coated with radium salt to provide fluorescent hands. As this process was common in the past, the results of the measurement fulfill expectations.

The unknown samples Sample 1 and Sample 2 could be assigned to known γ-spectra from the literature. Sample 1 is a substance containing ^{238}U, probably uranium ore.
Sample 2 was identified as containing thorium, possibly monazite phosphocei.

The measurement with the semiconductor detector can be used for a variety of purposes. For example, the radioactive nuclides that occur in an area can also be determined in the open due to the high accuracy. A more pragmatic application can be found in the analysis of mineral samples and metals. These can be used to draw conclusions about the composition of the soil at great depths and to search for resource deposits. Uranium and pitchblende are particularly worth mentioning here.

The age and geographical origin of a sample with a known composition can also be determined on the basis of characteristic radioactive nuclides, which offers great potential for historians and geologists.

Literature used

[1] *Alibaba online store*. url: https://german .alibaba.com /g/monazite- powder .html. (as of 22.10.2021).

[2] Inc. Canberra Industries. "DSA-1000 Digital Spectrum Analyzer Hardware Manual". In: (2005). url: https://home.uni-leipzig.de/physfp/manuals/DSA-1000%20Hardware%20Manual.pdf. (as of 22.10.2021).

[3] *Chemistry at school*. url: https://www.chids.de/dachs/expvortr/642/LumiDateien/radio.html. (as of: 24.10.2021).

[4] Wolfgang Demtröder. *Atoms, molecules and solids*. Experimental Physics 3. Springer-Verlag, 2010. isbn: 978-3-642-03910-2.

[5] A. King. "Gamma spectra of the 234, 235, and 238 uranium isotopes." In: (1976). doi: 10.2172/7363085. url: https://www.osti.gov/biblio/7363085. (as of 22.10.2021).

[6] *Leifiphysics, experiments on gamma spectroscopy*. URL: https :// www . leifiphysik . de / nuclear-particle-physics/radioactivity-continuation/experiments/further%20e-gamma-spectra. (as of 19.10.2021).

[7] H. Lohninger. *Thorium*. URL: http :// inorganic . chemistry . vias . org / thorium . html. (as of 22.10.2021).

[8] University of Leipzig. Faculty of Physics and Meterology. F practical course. Dr. M. Lorenz. "High-resolution-gamma spectroscopy with a Ge-semiconductor detector". In: (1999). URL: https : / / home . uni - leipzig . de / physfp / manuals / Gamma _ HP _ d _ e . pdf. (as of 22.10.2021).

[9] Bee Research. *Th232-spectrum*. URL: https://www.gammaspectacular.com/blue/th232-spectrum. (as of 22.10.2021).

[10] Uwe Spillmann. "Characterization and first experimental use of spatially resolving, energy-dispersive germanium detectors for precision spectroscopy of heavy ions". In: (2009). url: https://core.ac.uk/download/pdf/14506169.pdf. (as of 22.10.2021).